Solitonlike Electromagnetic Waves behind a Superintense Laser Pulse in a Plasma

S. V. Bulanov,[1,*] T. Zh. Esirkepov,[2,†] N. M. Naumova,[2,*] F. Pegoraro,[3] and V. A. Vshivkov[2,‡]

[1]*Scuola Normale Superiore, Pisa, Italy*
[2]*Forum for Theoretical Physics INFM, Pisa, Italy*
[3]*Dipartimento di Fisica, Università di Pisa and INFM, Pisa, Italy*

(Received 18 May 1998)

We present strong evidence, based on 2(1/2)D particle-in-cell simulations of the interaction of ultrashort, high-intensity laser pulses with underdense plasmas, of the formation of long-lived, slowly moving $(0.1c)$, low-frequency solitonlike electromagnetic waves. These nonlinear waves consist of electron-density depressions and intense cylindrical electromagnetic field concentrations with a larger amplitude and a lower frequency than those of the laser pulse. [S0031-9007(99)09029-8]

PACS numbers: 52.40.Nk, 52.35.Sb, 52.60.+h, 52.65.Rr

Depending on the pulse and plasma parameters, the energy of ultrashort, high-intensity laser pulses [1] can be transferred to various nonlinear collective plasma excitations. The energy of a laser pulse propagating in an underdense plasma is converted into high-frequency electromagnetic waves [2] and into electrostatic wake waves, generating in this process beams of fast electrons [3]. These produce a quasistatic magnetic field [4] and electron fluid vortices [5]. Both the wake fields and the magnetic field vortices stay in the plasma much longer than the laser pulse because of the very low propagation velocity of their energy density. We show that, in addition, long-lived solitonlike nonlinear waves are formed and remain in the plasma behind the laser pulse.

Among nonlinear modes, solitons are of fundamental importance for basic nonlinear science [6]. In Ref. [7], fast solitons propagating in a plasma with group velocity close to the speed of light were invoked as a tool for particle and photon acceleration. Nonlinear one-dimensional (1D) relativistic solitons were studied analytically [7–9] and numerically [9–11]. It was shown in computer simulations and analytically [9] that, in the 1D case, the width of the solitons generated by a laser pulse in an underdense plasma is of the order of the skin depth and that their propagation velocity is much smaller than the group velocity of the laser light. Two-dimensional, localized, nonlinear electromagnetic structures were observed in simulations with inhomogeneous plasmas near the critical density [12]. With the strong localization of the electromagnetic fields at the plasma resonance region in these so-called "bubbles," their amplitude and width depended (as well as on the amplitude of the wave and on nonlinear or dissipative effects) principally on the scale of the plasma inhomogeneity and require a weakly nonlinear wave. In our case, however, the solitonlike waves are formed in homogeneous plasmas in the limit of strong nonlinearity. An analogy can be found between the solitary waves reported in this paper and the evacuated channels formed during pulse self-focusing (studied in Refs. [13] and [14]). However, in the latter case, the channels are elongated in the direction of the laser beam and are mainly axially polarized (along x), while we observe structures that are equally confined in x and y and are polarized as the laser pulse.

In this Letter we study relativistic solitonlike waves with the help of 2D particle-in-cell numerical simulations and show that they are formed during the laser pulse plasma interaction. Simulations are performed with a fully relativistic code developed at the Institute of Computational Technologies in Novosibirsk and at the Forum for Theoretical Physics INFM, Scuola Normale Superiore, Pisa. The size of the simulation box is 125λ along x (the direction of the laser pulse propagation) and 40λ along y (transverse direction). The cell size is $(1/12 \times 1/12)\lambda^2$ with about 10 particles per cell. The total number of particles is approximately 6×10^6. The plasma begins at $x = 0$ and is preceded by a vacuum region 5λ long. The laser pulse is initialized outside the plasma in the vacuum region $x < 0$. In the first run shown here, the dimensionless amplitude of the laser radiation is $a = eE/m\omega c = 3$ (which corresponds to the intensity $I \approx 2 \times 10^{19}$ W/cm^2 for 1 μm wavelength). The laser pulse has a Gaussian form in both the x and the y directions, with full width $l_\perp = 5\lambda$ and length $l_\parallel = 12\lambda$, corresponding to a 40 femtosecond pulse length at 1 μm wavelength, and is linearly s polarized with its incident electric field along the z axis. In the simulations presented here, ions are assumed to be fixed. The plasma density is $n_0 = 0.2025 n_{\rm cr}$, where $n_{\rm cr} = \omega^2 m/4\pi e^2$ is the critical density. The corresponding ratio between the plasma period and the period of the laser radiation is 2.222. The laser pulse power $P = a^2 l_\perp$ is above the threshold for relativistic filamentation (see, e.g., Ref. [13]).

Because of self-focusing, the laser pulse amplitude reaches its maximum value, $a \approx 7$, on the axis at $t = 30$. At $t = 60$ filamentation occurs with the formation of an intense filament on the axis and of two weaker symmetric lateral filaments. At $t \approx 100$ the laser pulse has lost approximately half of its initial energy.

The distribution of the square root of the electromagnetic energy density, $W(x, y) = (\mathbf{E}^2 + \mathbf{B}^2)/8\pi$, in the x-y plane at $t = 120$ is shown in Fig. 1(a). Here space scales are normalized on λ and time on $2\pi/\omega$.

 0031-9007/99/82(17)/3440(4)$15.00 © 1999 The American Physical Society

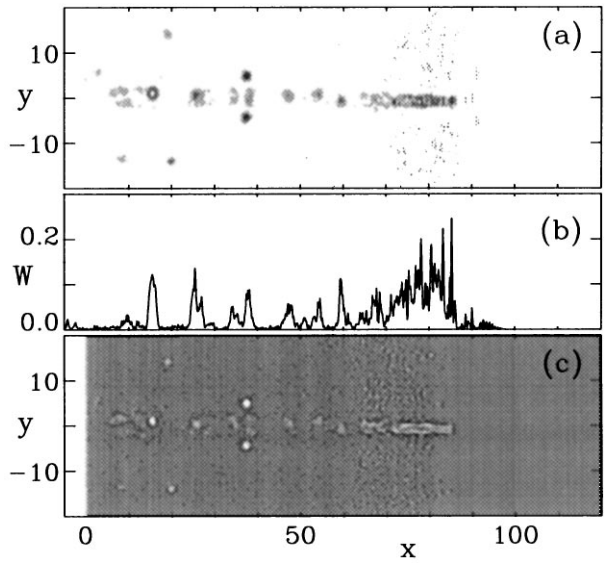

FIG. 1. Solitary waves in the $(x\text{-}y)$ plane behind a pulse with amplitude $a = 3$, width 5λ, and length 10λ in a plasma with $n/n_{\rm cr} = 0.2025$ at $\omega t/2\pi = 120$. (a) Distribution of the square root of the electromagnetic energy density in the $(x\text{-}y)$ plane; (b) electromagnetic energy density on the axis versus x; (c) electron density marking the solitary waves.

In the region $80 < x < 100$ we see that the form of the pulse has changed due to self-focusing and energy depletion. Behind the pulse, about ten spots of high electromagnetic energy density are seen, which we identify as *slow solitonlike waves*. Their propagation velocity is much smaller than the group velocity of the laser light, as shown by the solitary wave which remains at $x \approx 14$, $y \approx 1$ for about 135 laser periods. In Fig. 1(a) the square root of $W(x, y)$ is plotted to enhance smaller solitary waves. We also see the ribbonlike regions with a strong quasistatic magnetic field studied in Ref. [5]. The relative amplitude of the electromagnetic structures of the electromagnetic energy density on the pulse axis, $W(x, y = 0)$, is given by the plot in Fig. 1(b). In Fig. 1(c) the distribution of the electron density is presented. We see a low-density region corresponding to the laser pulse position and additional low-density regions corresponding to the solitary waves. The solitary waves are located mainly along the path of the laser pulse propagation. The pair of "lateral" solitary waves with coordinates $x \approx 38$, $y \approx \pm 4$ has been generated at $t = 60$ by the two lateral filaments. Later, these filaments decayed while the solitary waves lasted. From these numerical results we see that the typical size of the solitary waves is $\approx 2\lambda$ to 4λ, i.e., comparable to the Langmuir wavelength, $\lambda_p = c/\omega_{\rm pe} = 2.2\lambda$. The time dependence of the z component of the electric field inside the solitary waves shows oscillations with a period ≈ 3 to 4 times the laser pulse period which is longer than the period of the Langmuir wave $2\pi/\omega_{\rm pe}$.

In order to illustrate the observed structure of the electromagnetic field and electron density in these solitary waves, we assume that their propagation speed is zero, and consider cylindrically symmetric configurations, where all variables depend on the r coordinate. Here we use the approach formulated in Ref. [13] and developed in Ref. [14]. We use the equations of motion for a cold electron fluid together with Maxwell's equations. The z component of the electric field oscillates in time while the electron-density distribution remains constant. The radial component of the ponderomotive force $\langle \mathbf{j} \times \mathbf{B} \rangle$, which leads to the density redistribution, is balanced by the electric force due to the charge separation. Then, the normalized electron density is $n(r) = 1 + \varepsilon^2 \Delta_\perp \langle \sqrt{1 + a^2} \rangle$, where $\varepsilon = \omega_{\rm pe}/\omega$ and $\Delta_\perp = r^{-1} \partial_r r \partial_r$. Assuming that the time dependence of the vector potential has the form $a(r) \exp[-i(1 - \delta\omega)t]$, in the limit of weak nonlinearity $a < 1$ from Eq. (19) of Ref. [13], we find

$$\varepsilon^2 \Delta_\perp a - (2\delta\omega - |a|^2) a = 0, \qquad (1)$$

where $\delta\omega$ is the nonlinear frequency shift. The properties of this equation are well known. It describes localized 2D solitary waves with frequency shift $\delta\omega$ and radius r_0 which depend on the soliton amplitude. It is known that Eq. (1) predicts instability of the localized solution [6]. For relativistically strong electromagnetic solitary waves, this equation is modified by contributions to Eq. (1) of higher order in a^2 and $\Delta_\perp a^2$, arising from the expansion of the $\sqrt{1 + a^2}$ terms in the density and in the electron velocity response, which changes its stability property. Our simulation results indicate that sufficiently large amplitude solitary waves are stable. The same scaling has been obtained in Ref. [9] for a plane 1D soliton with circularly polarized electromagnetic radiation trapped inside it. As was proved in [9], the problem of a plane 1D soliton admits an exact analytical solution. This solution shows that in the weak nonlinearity limit $\delta\omega \sim a^2$ and $r_0 \sim \varepsilon/a$, while in the ultrarelativistic limit, the width r_0 depends on the solitary wave amplitude as $r_0 \sim \varepsilon/\sqrt{a}$ and that its frequency decreases as $\omega \sim 1/\sqrt{a}$.

The increase of the period T of the solitary waves of Fig. 1 with their maximum amplitude a_m, is shown in Table I, where (s-polarized) solitary waves behind the narrow laser pulse are identified by their position in the $x\text{-}y$ plane at $t \approx 100$. Note that all of the listed solitary waves have amplitudes larger than 1 because they are easier to resolve and because of their enhanced stability.

The physical mechanism for the generation of these solitary waves is different from the standard process, where the nonlinear steepening of the wave increases up to the stage when it is counterbalanced by the effect of dispersion, and is based on the frequency downshift of the laser pulse. This downshift is similar to that discussed in Refs. [10,11,15] and appears because of the energy depletion of the laser pulse. The pulse depletion length [16] $l_{\rm depl} \approx l_{\rm pulse}(\omega/\omega_{\rm pe})^2 \approx 10$ for the parameters of our simulation, in agreement with the distance where the first soliton is generated. On the other hand, the group velocity of the laser pulse decreases as the carrier frequency

TABLE I. Position, amplitude, and period of the solitary waves.

N_0	x	y	a_m	T
1	14	+1	7.9 ± 0.1	4 ± 0.1
2	20	+14	2.0 ± 0.25	2.5 ± 0.2
3	20	−14	2.2 ± 0.3	2.5 ± 0.1
4	30	−2	7.0 ± 0.5	3.8 ± 0.4
5	32	+1	6.5 ± 2.5	2.7 ± 0.5
6	38	+4	5.3 ± 1	3.1 ± 0.2
7	38	−4	5.9 ± 1	3.0 ± 0.1
8	47	+2	6.0 ± 2	3.6 ± 0.6
9	55	+1	7.6 ± 1.5	3.5 ± 0.5

is downshifted. Thus the depleted portions of the pulse, e.g., inside the lateral filaments, lag behind and convert their energy into solitary waves with small group velocity.

Wider laser pulses produce a cloud of solitary waves in their wake. This is shown in Fig. 2 for an s-polarized pulse with amplitude $a = 3$, width 30λ, and length 5λ in an underdense plasma ($n/n_{cr} = 0.2025$). At $t = 80$ we see about 25 solitary waves behind the laser pulse. Many of them have amplitudes larger than the laser pulse. Their initial positions along y correspond to the position of the laser radiation filaments. Afterwards, the solitary waves move along x and toward the laser pulse axis with typical velocity $\approx 0.1c$. In the case of both narrow and wide pulses the typical solitary wave amplitude ranges up to $a \gg 1$, and their frequency and width are in the range $(1/3)\omega$ to $(1/4)\omega$ and 2λ to 3λ, respectively.

Solitary wave formation is also observed for wide p-polarized pulses with the incident electric field in the x-y plane. However, p-polarized solitary waves are not as distinctive as s-polarized solitary waves because of the more turbulent plasma conditions and because of the interference with the pulse electric field along y and with the quasistatic magnetic field generated by fast particles [5] along z. The structure of s- and p-solitary waves, as obtained from Eq. (1) and from its generalization to p-solitary waves, is shown in Figs. 3(a) and 3(b), respectively. The distribution of the electron density, of the E_z (E_φ) component of the electric field and of the B_φ (B_z) component of the magnetic field are shown for s (p) polarized solitary waves. In Fig. 3(c) the corresponding quantities are shown for the s-polarized solitary wave located at $x \approx 14$, $y \approx 1$ in the simulation shown in Fig. 1 and, in Fig. 3(d), for a p-polarized solitary wave located at $x \approx 19$, $y \approx 3$ behind a wide p pulse with the same parameters as in Fig. 2. We see that there is agreement between the theoretical model and simulation results.

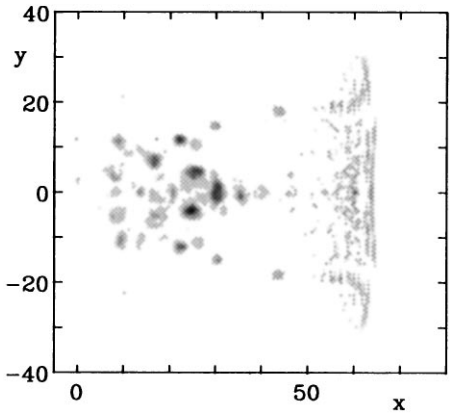

FIG. 2. Distribution of the square root of the electromagnetic energy density in the (x-y) plane showing the cloud of solitary waves generated behind a wide s-polarized laser pulse with amplitude $a = 3$, width 30λ, and length 5λ in a plasma with $n/n_{cr} = 0.2025$ at $\omega t/2\pi = 80$.

In Fig. 4 the two-dimensional reconstruction of the z component of the electric field of the s-polarized solitary wave of Fig. 1(a) at $x \approx 20$, $y \approx -14$ is shown in Fig. 4(a) at $t = 106$. In Fig. 4(b) the corresponding density contours and the vector plot of the magnetic field in the x-y plane versus time are shown at $t = 105$. In Fig. 4(c) the time dependence of the maximum positive and negative values of the momentum along z of the different electrons inside the solitary wave is shown. The central band is due to electron heating. These values correspond to a vector potential of order $a \approx 2.25$. The frequency of the momentum oscillations is about 2.5 times smaller than the laser frequency and about 1.125 times smaller than the Langmuir frequency in the plasma far from the solitary wave. Thus, the corresponding E_z component of the electric field

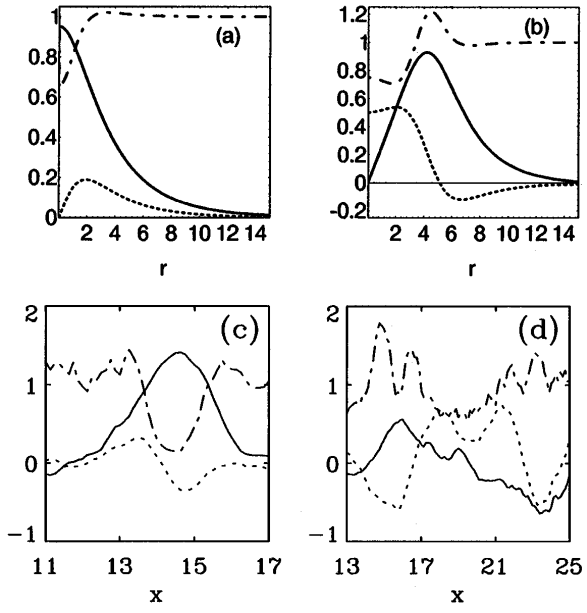

FIG. 3. (a) Analytical distribution of the electric field E_z (solid line), of the magnetic field B_φ (dotted line), and of the electron density n (dash-dotted line) inside an s-polarized solitary wave with $E_z(0) = 0.915$ and $\delta\omega = 0.03675$. (b) The corresponding quantities, B_z (dotted line), E_φ (solid line), and n (dash-dotted line) for a p-polarized solitary wave with $B_z(0) = 0.5$ and $\delta\omega = 0.07025$. (c) The same quantities for the s-solitary wave at $x \approx 14$, $y \approx 1$ in the numerical simulations of Fig. 1. (d) The same quantities for the p-solitary wave at $x \approx 19$, $y \approx 3$ behind a wide p-polarized pulse.

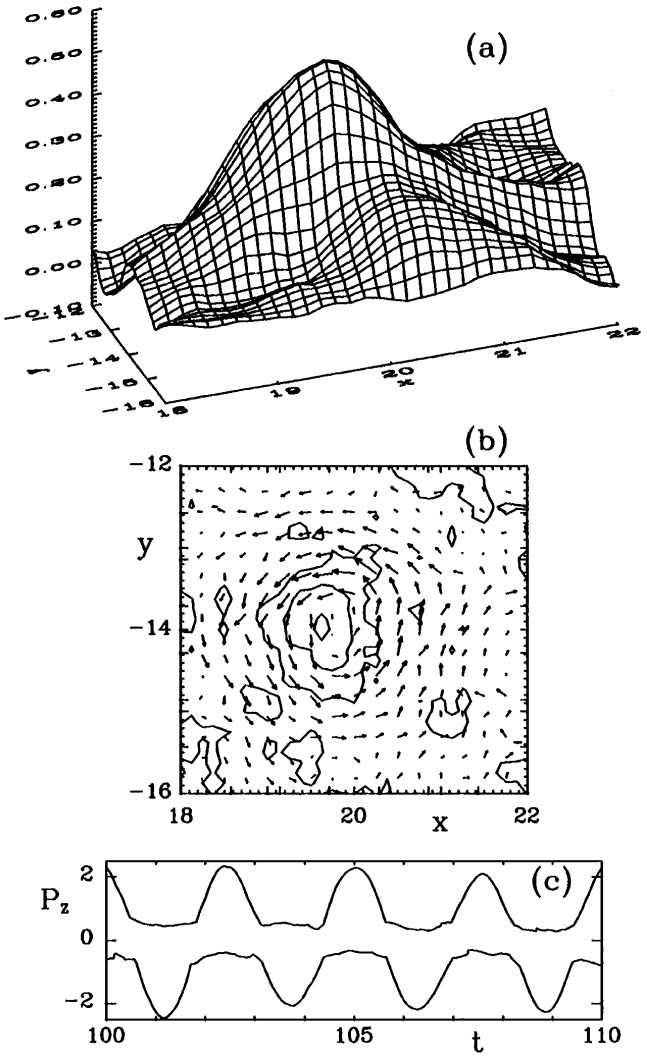

FIG. 4. (a) 2D plot in the x-y plane of E_z inside the s-polarized solitary wave of Fig. 1(a) at $x \approx 20$, $y \approx -14$ at $\omega t/2\pi = 106$. (b) The corresponding density contours and the vector plot of the magnetic field at $\omega t/2\pi = 105$. (c) Time dependence of the maximum positive and negative values of the momentum along z of the different electrons inside the solitary wave.

is about 0.9. Estimating the amount of energy contained in the solitary wave in the wake of the wide pulse in Fig. 2, we obtain that at $t = 80$, when the laser pulse has lost almost all of its initial energy, about 30% to 40% of the pulse energy has been transformed into transversally oriented solitary waves. This fairly high efficiency of electromagnetic energy transformation demonstrates that the solitary waves play an important role in the description of the elementary structures, of which plasma turbulence is formed.

We are pleased to acknowledge the Scuola Normale Superiore of Pisa for the use of Origin 2000. We thank F. Califano for his help and interest in this work.

*Permanent address: General Physics Institute of RAS, Moscow, Russia.
†Permanent address: Moscow Institute of Physics and Technology, Dolgoprudnyi, Russia.
‡Permanent address: Institute of Computational Technologies of SD-RAS, Novosibirsk, Russia.

[1] G. Mourou, C. P. J. Barty, and M. D. Perry, Phys. Today **51**, No. 1, 22 (1998).
[2] C. D. Decker, W. Mori, and T. Katsouleas, Phys. Rev. E **50**, R3338 (1994); A. S. Sakharov and V. I. Kirsanov, Phys. Rev. E **49**, 3274 (1994); B. Quesnel, P. Mora, J. C. Adam, S. Guerin, A. Heron, and G. Laval, Phys. Rev. Lett. **78**, 2132 (1997).
[3] A. Modena *et al.*, Nature (London) **337**, 606 (1995); K. Nakajima *et al.*, Phys. Rev. Lett. **74**, 4428 (1995); R. Wagner, S. Chen, A. Maksimchuk, and D. Umstadter, Phys. Rev. Lett. **78**, 3125 (1997).
[4] D. W. Forslund, J. M. Kindel, W. B. Mori, C. Joshi, and J. M. Dawson, Phys. Rev. Lett. **54**, 558 (1985); G. A. Askar'yan, S. V. Bulanov, F. Pegoraro, and A. M. Pukhov, JETP Lett. **60**, 251 (1994); A. M. Pukhov and J. Meyer-ter-Vehn, Phys. Rev. Lett. **76**, 3975 (1996); R. J. Mason and M. Tabak, Phys. Rev. Lett. **80**, 524 (1998).
[5] S. V. Bulanov, M. Lontano, T. Zh. Esirkepov, F. Pegoraro, and A. M. Pukhov, Phys. Rev. Lett. **76**, 3562 (1996); S. V. Bulanov, T. Zh. Esirkepov, M. Lontano, and F. Pegoraro, Plasma Phys. Rep. **23**, 660 (1997).
[6] V. E. Zakharov, Sov. Phys. JETP **35**, 908 (1972); E. A. Kuznetsov, Chaos **6**, 381 (1996).
[7] K. Mima, T. Ohsuga, H. Takabe, K. Nishihara, T. Tajima, E. Zaidman, and W. Horton, Phys. Rev. Lett. **57**, 1421 (1986); T. Tajima, Nature (London) **327**, 285 (1987); P. K. Kaw, A. Sen, and T. Katsouleas, Phys. Rev. Lett. **68**, 3172 (1992).
[8] V. A. Kozlov, A. G. Litvak, and E. V. Suvorov, Sov. Phys. JETP **76**, 148 (1979); P. K. Shukla, M. Y. Yu, and N. L. Tsintsadze, Phys. Fluids **27**, 327 (1984); H. H. Kuehl, C. Y. Zhang, and T. Katsouleas, Phys. Rev. E **47**, 1249 (1993); V. I. Berezhiani and S. M. Mahajan, Phys. Rev. Lett. **73**, 1110 (1994).
[9] T. Zh. Esirkepov, F. F. Kamenets, S. V. Bulanov, and N. M. Naumova, JETP Lett. **68**, 36 (1998).
[10] S. V. Bulanov, I. N. Inovenkov, V. I. Kirsanov, N. M. Naumova, and A. S. Sakharov, Phys. Fluids B **4**, 1935 (1992).
[11] S. V. Bulanov, T. Zh. Esirkepov, F. F. Kamenets, and N. M. Naumova, Plasma Phys. Rep. **21**, 600 (1996).
[12] E. J. Valeo and K. G. Estabrook, Phys. Rev. Lett. **34**, 1004 (1975).
[13] G.-Z. Sun, E. Ott, Y. C. Lee, and P. Guzdar, Phys. Fluids **30**, 526 (1987).
[14] M. D. Feit, A. M. Komashko, S. L. Musher, A. M. Rubenchik, and K. S. Turitsyn, Phys. Rev. E **57**, 7122 (1998).
[15] W. Horton and T. Tajima, Phys. Rev. A **34**, 4110 (1986).
[16] S. V. Bulanov, I. N. Inovenkov, V. I. Kirsanov, N. M. Naumova, A. S. Sakharov, and H. A. Shakh, Phys. Scr. **47**, 209 (1993).